STEM CELLS AND DEVELOPMENT
Volume 31, Numbers 21–22, 2022

DOI: 10.1089/scd.2022.0091

Survival Motor Neuron Enhances Pluripotent Gene Expression and Facilitates Cell Reprogramming

Wei-Fang Chang,[1,*] Tzu-Ying Lin,[1,*] Min Peng,[1] Chia-Chun Chang,[1] Jie Xu,[2] Hsiu-Mei Hsieh-Li,[3] Ji-Long Liu,[4,5] and Li-Ying Sung[1,6,7]

Survival motor neuron (SMN) plays important roles in snRNP assembly and mRNA splicing. Deficiency of SMN causes spinal muscular atrophy (SMA), a leading genetic disease causing childhood mortality. Previous studies have shown that SMN regulates stem cell self-renewal and pluripotency in *Drosophila* and mouse and is abundantly expressed in mouse embryonic stem cells. However, whether SMN is required for establishment of pluripotency is unclear. In this study, we show that SMN is gradually upregulated in preimplantation mouse embryos and cultured cells undergoing cell reprogramming. Ectopic expression of SMN increased cell reprogramming efficiency, whereas knockdown of SMN impeded induced pluripotent stem cell (iPSC) colony formation. iPSCs could be derived from SMA model mice, but impairment in differentiation capacity may be present. The ectopic overexpression of SMN in iPSCs can upregulate the expression levels of some pluripotent genes and restore the neuronal differentiation capacity of SMA-iPSCs. Taken together, our findings not only demonstrate the functional relevance of SMN in establishment of cell pluripotency but also propose its potential application in facilitating iPSC derivation.

Keywords: survival motor neuron, spinal muscular atrophy, induced pluripotent stem cells, somatic cell reprogramming, neuronal differentiation

Introduction

Survival motor neuron (SMN), also known as Gemin1, is ubiquitously expressed in a wide range of cell types [1–3]. In cooperation with other proteins, SMN plays an important role in small nuclear ribonucleoprotein (snRNP) maturation and is the core component of the RNA spliceosome [4,5]. In addition to mRNA splicing, SMN participates in many other processes, including transcription initiation and termination, processing of the 3′ end of histone mRNAs, activation of telomerase, enhancing of RAD51-mediated homologous recombination, and sustaining R-loop-mediated genome stability [6].

Spinal muscular atrophy (SMA) is a neurodegenerative disorder caused by complete deletions or mutations of the *SMN1* gene. Deficiency of the SMN protein and consequently loss of α-motor neurons in the spinal cord can lead to progressive proximal muscle weakness and paralysis [7,8]. The incidence of SMA is about 1 in 6,000–10,000 live births, while the prevalence of the SMA carrier is 1 in 40–50 [9,10].

SMA is commonly divided into four types: (1) SMA type I (Werdnig–Hoffmann disease; infantile SMA) is the most severe type, with onset time between birth and 6 months, and patients generally die before age 2; (2) SMA type II (Dubowitz disease; intermediate SMA) affects children aged 6 to 18 months and the common symptoms

[1]Institute of Biotechnology, National Taiwan University, Taipei, Taiwan.
[2]Center for Advanced Models for Translational Sciences and Therapeutics, University of Michigan Medical Center, Ann Arbor, Michigan, USA.
[3]Department of Life Science, National Taiwan Normal University, Taipei, Taiwan.
[4]MRC Functional Genomics Unit, Department of Physiology, Anatomy and Genetics, University of Oxford, Oxford, United Kingdom.
[5]School of Life Science and Technology, ShanghaiTech University, Shanghai, China.
[6]Agricultural Biotechnology Research Center, Academia Sinica, Taipei, Taiwan.
[7]Animal Resource Center, National Taiwan University, Taipei, Taiwan.
*Cofirst author.

include difficulty in walking and respiratory problems; (3) SMA type III (Kugelberg–Welander disease; juvenile SMA) usually manifests 12 months after birth and patient life span is usually unaffected, and patients can walk with or without support, but with trouble running or climbing stairs; and (4) SMA type IV (adult-onset SMA), or the late-onset SMA type III, usually occurs in adulthood with symptoms such as weakening of proximal muscles of the extremities.

Several SMA animal models, including *Caenorhabditis elegans* [11,12], *Drosophila melanogaster* [13,14], *Danio rerio* [15,16], and *Mus musculus* [17–19], have been established for preclinical researches. The SMA mouse model is generated by introducing human *SMN2* into the genome of an *Smn1*-null mouse. These SMA mice may manifest different severity levels of pathological phenotypes, ranging from undetectable mild symptoms (type III) to severe symptoms (type I) [17–19]. These animal models have been used to develop a clinical drug named Spinraza (nusinersen). More recently, an SMA oral drug was developed by Roche [20–22] and an adeno-associated virus (AAV) 9-based gene therapy is undergoing testing [23].

In our previous study, we have shown that SMN is highly expressed in mouse embryonic stem cells (mESCs) and spermatogonia stem cells (SSCs) [24,25]. Knockdown of *Smn1* in mESCs causes impaired pluripotent gene expression, activation of the ERK pathway (phospho-mitogen-activated protein kinase 1/2, phospho-p44/42 MAPK, p-ERK1/2), and decreased neuronal differentiation capacity.

Conversely, overexpression of *Smn1* suppresses ESC differentiation under treatment with retinoic acid (RA) [24]. In mouse SSCs, knockdown of *Smn1* leads to decreased expression of spermatogonia markers and compromised regeneration capacity after transplantation. Abnormalities in gamete development and the loss of spermatogonia markers were frequently observed in SMA-like mice [25].

SMA patient-derived human induced pluripotent stem cells (iPSCs) have been established in 2009 and correction of mutant SMN genes restored the capacity for neuronal differentiation [26–29]. Some studies reveal that additional expression of Lin28 and p53 shRNA enhances cell reprogramming of fibroblasts from SMA patients, suggesting that apoptosis occurs more frequently in early reprogramming of SMN-deficient cells [26,27,29].

In this study, we demonstrate that the expression of SMN gradually increases in preimplantation mouse embryos. During induced cell reprogramming, the SMN level correlates with the expression of endogenous pluripotent genes. Overexpression and knockdown of SMN render increased and decreased cell reprogramming efficiency, respectively. In SMA mouse iPSCs, the ectopic expression of exogenous SMN significantly increases expression levels of some pluripotent genes and restores the defects in neuronal differentiation in vitro.

Our findings show that the SMN expression level is highly correlated with pluripotent gene expression and cell reprogramming efficiency.

Materials and Methods

Animals

All animal maintenance and care procedures were reviewed and approved by the Institutional Animal Care and Use Committee (IACUC) of National Taiwan University according to the protocol numbers, NTU-105-EL-68 and NTU-107-EL-154. C57BL/6 strain mice were purchased from the National Laboratory Animal Center (NLAC) (Taipei, Taiwan). To obtain the SMA mouse model, we purchased the $Smn1^{hung+/-}$; $SMN2Hung^{tg/tg}$ mice, which were established by Dr. Hung Li's group and were contributed to NLAC [18].

We intercrossed SMA mice carrying a hemizygous for the *SMN2Hung* transgene ($SMN2Hung^{tg/-}$) and heterozygous for the *Smn1* ($Smn1^{+/-}$) target mutation to yield progeny with different phenotypes, including the type I severe type ($Smn1^{hung-/-}$; $SMN2Hung^{tg/-}$), intermediate type ($Smn1^{hung-/-}$; $SMN2Hung^{tg/tg}$), and milder type, within the same litter.

Cell culture

The pluripotent R1 ESC line (129/Sv × 129/Sv-CP) [30] was maintained on mouse embryonic fibroblast (MEF) feeder layers coated with 0.1% gelatin (ES-006-B, Millipore, Darmstadt, Germany) and cultured in Dulbecco's modified Eagle's medium (DMEM; 11995065; Thermo, Carlsbad, CA, USA) supplemented with 15% fetal bovine serum (FBS; SH30071.03; Hyclone, Logan, UT, USA), 1 × nonessential amino acid (NEAA; 11140050; Thermo), 1 × β-mercaptoethanol (β-ME; ES0070E; Millipore), 2 mM GlutaMax (35050061; Thermo), 1 × penicillin/streptomycin (P/S; 15140122; Thermo), and 1,000 U/mL ESGRO (ESG1106; Millipore).

iPSCs were cultured in KnockOut DMEM (KO-DMEM; 10829-018; Thermo) supplemented with 15% KnockOut Serum Replacement (KSR; 10828028; Thermo) and ESGRO for sustaining pluripotency.

To establish adult tail-tip fibroblasts (TTFs), the tail tissues from adult SMA mice were minced and covered with a glass coverslip in the culture with 10% FBS/DMEM (MEF medium) for 5–7 days. Cells that migrated out from tissues were transferred to new plates. TTFs at passage 3 or 4 were used for iPSC derivation.

For the growth curves of iPSCs, cells (1×10^5) were seeded into each well of six-well plates. Triplicate wells were harvested by trypsinization and counted using a hemacytometer at the indicated time points.

Retrovirus and lentivirus production

iPSCs were generated from C57/BL6 MEFs or SMA-TTFs by retroviral or lentiviral infection. For retrovirus production, Plat-E cells [31] were maintained in DMEM containing 10% FBS, 1 μg/mL puromycin (ant-pr-1, InvivoGen), 10 μg/mL blasticidin S (Funakoshi), penicillin, and streptomycin by routine passage with 0.05% trypsin–ethylenediaminetetraacetic acid (EDTA). One day before transfection, Plat-E cells were passaged and seeded at 3×10^6 cells per 100-mm culture dish without puromycin and blasticidin.

The pMX-based *Oct4/Pou5f1*, *Sox2*, *Klf4*, and *cMyc* (OSKM) plasmid donated by Yamanaka's group (plasmid ID: 13366, 13367, 13370, 13375, and 22724) was obtained from Addgene [32,33]. shLacZ and shSMN plasmids carrying a puromycin resistance gene were purchased from the National RNAi Core Facility (shLacZ: TRCN0000072224;

shSMN: TRCN0000072018). All DNA plasmids were introduced into Plat-E cells at 50%–60% cell confluence after 16–24 h of culture, using the jetPRIME Transfection Reagent (114–15, Polyplus-transfection; Illkirch, Strasbourg, France). Briefly, 10 μg of DNA plasmids and 20 μL of transfection reagent were mixed with 0.5 mL of jetPRIME buffer and incubated for 10 min at room temperature.

After incubation, the DNA/transfection reagent mixture was added gently and dropwise into Plat-E cell culture media and cultured at 37°C with 5% carbon dioxide. Culture media were changed after 16 h. The virus-containing supernatants were harvested at 48 h after transfection and filtered through a 0.45-mm cellulose acetate filter and were ready for target cell infection.

For lentiviral collection, an additional harvest at 72 h after transfection was performed, and these harvested supernatants were filtered, mixed with the TOOLSilent Lenti-Precipitating Reagent (VCT-K00, TOOLS Biotechnology, Taiwan) to concentrate, and resuspended using cold KO-DMEM in 1/100 of the original volume. The 100× lentiviral media were used fresh or aliquoted and stored at −80°C until use.

Generation of induced pluripotent stem cells

For target cell infection, MEFs were infected with the OSKM retrovirus for an equal volume supplemented with 8 μg/mL polybrene (H9268; Sigma) at 1×10^5 cells in a six-well dish on the seeding day, while TTFs were seeded 1 day before infection. After 2 days of retroviral infection, the culture medium was then replaced with MEF medium for 3 days and changed to iPSC medium at 5 dpi. The media were changed every 2 days.

Target cells were replated on feeder layers at 2×10^5 cells per six-well dish at 7 dpi. RNA and protein from 7, 14, 21, and 28 dpi cells were collected for real-time polymerase chain reaction (RT-PCR) and western blot analysis. Colony formation efficiency of iPSCs was determined by alkaline phosphatase (AP) staining (SK-5300; Vector Laboratories, Burlingame, CA, USA) at 28 dpi, following the manufacturer's instructions.

To establish a stable iPSC line, colonies were manually picked up into a 96-well plate individually for further 3 days of culture. Colonies were dissociated into single cells by 0.25% trypsin/EDTA digestion for 3 min, neutralized with ESC medium, and seeded in a 24-well dish. For each mouse, two iPSC clones were derived for biological replicates used for the RT-PCR, western blot analysis, and growth curve.

Infection of MEFs with SMN overexpression lentivirus

To generate an *Smn1*-overexpressing plasmid, a mouse *Smn1* coding sequence was cloned into pSin-EF2-Oct4-Pur (plasmid No. 16579; obtained from Addgene) by replacing the human *OCT4* gene. Lentivirus was produced by transfection of an empty vector (vector control, vc) and overexpression of SMN (ovSMN) plasmids into Plat-E cells and concentrated for further infection.

For B6 MEFs, the vector control and *Smn1*-overexpressing lentivirus were mixed with the OSKM retrovirus for iPSC generation. For established iPSC lines, puromycin (2 μg/mL, ant-pr-1; InvivoGen, Pak Shek Kok, Hong Kong) was used for antibiotic selection after 3 dpi.

In vitro differentiation

The method of in vitro neuronal lineage differentiation was performed according to the system established by Thomas M. Jessel's group [34] with modifications. For step 1, trypsinized iPSCs were plated at 3.7×10^5 cells per 60-mm Petri dish and cultured in 15% KSR/KO-DMEM without ESGRO for 2 days to form embryoid bodies (EBs).

For steps 2 and 3, the medium was changed into DFK5 medium comprising 66.75% DMEM, 23.75% Ham's F-12 nutrient mixture (F-12, 11765054; Thermo), 5% KSR, NEAA, β-ME, P/S, 1 mM GlutaMax, insulin–transferrin–selenium G supplement (ITS; 41400045; Thermo), B-27 supplement (17504044; Thermo), and 2 μM retinoic acid (RA, R2625; Sigma, St. Louis, MO, USA) till day 8.

Sonic hedgehog (Shh, 0.6 μg/mL, R&D, Minneapolis, MN, USA) was added to the DFK5 medium in the final step from day 9 to 11. EBs were collected for western blotting analysis at different time points.

RNA extraction and reverse transcription-PCR

Total RNA was purified with Azol RNA Isolation Reagent (Azol.200, ARROWTEC, New Taipei City, Taiwan) according to the manufacturer's instructions. For complementary DNA synthesis, total RNA was used for the reverse transcription reaction using the SuperScript III First-Strand Synthesis System supplemented with a random hexamer (18080051; Thermo), according to the manufacturer's instructions.

Semiquantitative PCR and RT-PCR (qPCR)

Semiquantitative PCR was performed with *GoTaq* polymerase (M3005; Promega, Madison, WI, USA). For RT-PCR, SYBR Green PCR master mix (KK4603, Kapa Biosystems, Inc., Woburn, MA, USA) was mixed with cDNA (25 ng) and forward/reverse primers to a final volume of 10 μL. RT-PCR was conducted using the Roche Light-Cycler (LC480, Roche Applied Science, Mannheim, Germany); the reaction condition was 15 s at 95°C and 30 s at 60°C for 45 cycles.

Amplification specificity was verified with melting curve analysis. *Gapdh* served as the internal control and was used for normalization of all RNA samples.

Western blot

Cultured cells were trypsinized, washed with ice-cold D-phosphate-buffered saline (PBS) twice, and lysed in an adequate volume of 1×RIPA buffer inhibitor (RIPA, Millipore) containing the proteinase inhibitor, followed by 10 min of standing at 4°C for cell lysis. Samples were then centrifuged at 16,000 *g* for 10 min at 4°C and the supernatant of each sample was collected and denatured at 95–100°C for 10 min. Samples were run on a 12% sodium dodecyl sulfate-polyacrylamide gel electrophoresis and transferred to a polyvinylidene fluoride membrane. The membrane was blocked for 30 min with 5% skimmed milk in PBS at room temperature.

The primary antibodies, mouse anti-SMN monoclonal antibody (0.05 μg/mL, 610646; BD Biosciences, San Jose, CA, USA); mouse anti-OCT4 monoclonal antibody (0.08 μg/mL, sc-5279; Santa Cruz Biotechnology, Inc., Dallas, TX, USA); rabbit anti-SOX2 polyclonal antibody (0.34 μg/mL, GTX101507; GeneTex, Hsinchu, Taiwan); rabbit anti-NANOG polyclonal antibody (0.04 μg/mL, RCAB002P-F; ReproCell Inc., Yokohama, Japan); mouse anti-SALL4 monoclonal antibody (0.05 μg/mL, H00057167-M03; Abnova, Taipei, Taiwan); rat anti-CD90/THY1 monoclonal antibody (0.2 μg/mL, 30-H12; Abcam, Boston, MA, USA); rabbit anti-PAX6 polyclonal antibody (0.5 μg/mL, GTX113241; GeneTex); mouse anti-βIII-TUBULIN monoclonal antibody (TUJ1; 1 μg/mL, MAB1637; Millipore); and mouse anti-α-TUBULIN monoclonal antibody (0.3 μg/mL, T5168; Sigma), were used for immunoblotting.

Membranes were incubated with primary antibodies at 4°C overnight. After incubation, membranes were washed with PBST and incubated with secondary antibodies for 1.5 h at room temperature.

The secondary antibodies, goat anti-mouse, rabbit, and rat IgG HRP-conjugated polyclonal antibodies (0.08 μg/mL, 31430, 31460, 31470; Thermo), were used. For signal development, membranes were applied with the T-Pro LumiFast Plus Chemiluminescent Substrate Kit (JT96-K002; T-Pro Biotechnology, New Taipei County, Taiwan) according to the manufacturer's instructions.

The light signal was detected using the GeneGnome XRQ chemiluminescence imaging system (SynGene, Cambridge, United Kingdom). α-TUBULIN served as the internal control and was used for normalization of all signals.

Immunofluorescence staining and confocal microscopy

Mouse embryos were fixed with 4% paraformaldehyde and washed with PBS. Permeabilization and blocking were achieved with 2.5% bovine serum albumin in Tris-buffered saline solution supplemented with 0.5% Triton X-100 for 30 min. The samples were incubated with primary antibodies at 4°C overnight and washed with PBST three times.

Subsequently, secondary antibodies conjugated with a fluorescent dye were used to incubate embryos at room temperature for 2 h. 4′,6-Diamidino-2-phenylindole (100 ng/mL, D9564; Sigma) was supplemented in the secondary antibody incubation. Mouse anti-SMN monoclonal antibody (1.25 μg/mL) and Alexa Fluor 488 goat anti-mouse IgG (A11029, 4 μg/mL, Thermo) were used.

After incubation with secondary antibodies, embryos were placed on slides and observed under a confocal microscope (TCS SP5 II, Leica, Wetzlar, Germany).

Statistics

The number of AP-positive iPSC colonies was analyzed and counted using ImageJ software. All data are presented as mean ± standard error of the mean and analyzed using Student's *t*-test or one-way ANOVA with Tukey's multiple comparison test (GraphPad Software Inc., La Jolla, CA, USA). Significance was assumed at a P value of 0.05.

Results

SMN is essential for somatic cell reprogramming

Many genes required for establishment and maintenance of pluripotency would be expressed in preimplantation embryos and during cell reprogramming [32]. SMN has been shown to be vital for stemness of mouse ESCs and SSCs, suggesting its role in preimplantation embryos and cell reprogramming. We first investigated the expression profile of SMN in mouse oocytes and preimplantation embryos (Fig. 1A, B).

SMN was expressed at a low level in germinal vesicle oocytes, which surged at the MII stage. After fertilization, however, the level of SMN dropped dramatically at the two-cell stage. At the four-cell stage, the SMN protein level was slightly detectable, which gradually increased afterward.

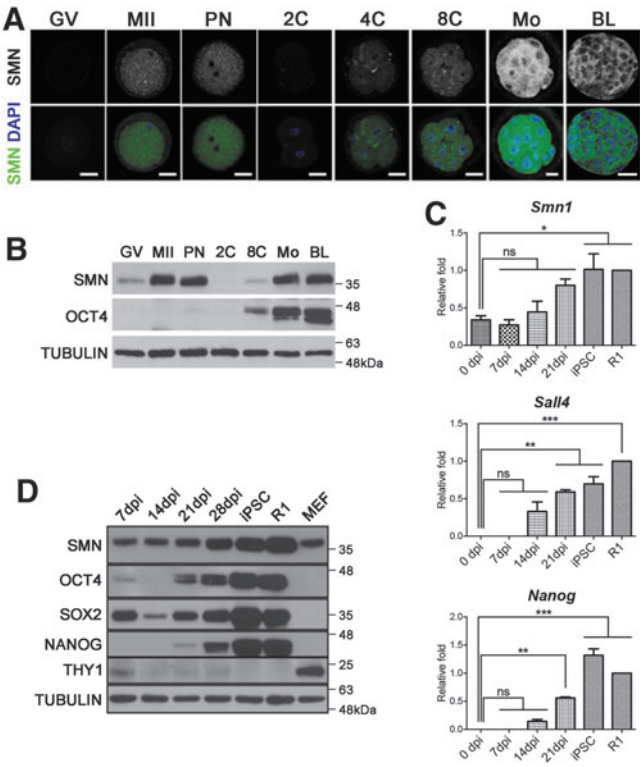

FIG. 1. SMN expression is upregulated along with pluripotent genes. **(A)** Immunofluorescence of mouse oocytes and preimplantation embryos for SMN (*green*) and DAPI (*blue*) at different stages. Scale bar = 25 μm. **(B)** Western blotting for SMN and OCT4 in mouse oocytes and preimplantation embryos. **(C)** RT-PCR for expression of *Smn1* and the pluripotent markers, *Sall4* and *Nanog*, in cells at different time points after reprogramming induction ($n = 3$) ($^{*}P < 0.05$, $^{**}P < 0.01$, and $^{***}P < 0.001$; Student's *t*-test). The R1 mouse ESCs and established iPSC clone at passage 10 (iPSC) are used as control. **(D)** Western blotting for SMN; pluripotent genes OCT4, SOX2, and NANOG; and THY 1, a marker for differentiated cells, in cells at different time points after reprogramming induction and R1 mouse ESCs. 2C, 2-cell; 4C, 4-cell; 8C, 8-cell; BL, blastocyst-stage embryos; DAPI, 4′,6-diamidino-2-phenylindole; ESC, embryonic stem cell; GV, germinal vesicle; iPSCs, induced pluripotent stem cells; MII, metaphase II oocyte; Mo, morula; PN, pronuclear; RT-PCR, real-time polymerase chain reaction; SMN, survival motor neuron.

Next, we sought to investigate expression patterns of SMN in somatic cells undergoing induced cell reprogramming. We reprogrammed MEFs, which were derived from a C57BL/6 mouse E13.5 fetus, by introducing exogenous *Oct4/Pou5f1*, *Sox2*, *Klf4*, and *cMyc* (OSKM, also dubbed as Yamanaka factors). SMN levels were subsequently determined at different reprogramming time points (7, 14, 21, and 28 dpi).

Semiquantitative RT-PCR and western blotting show that *Smn1* was expressed at low levels in MEFs, which gradually increased along with upregulation of pluripotent genes, including *Oct4*, *Sox2*, *Nanog*, and *Sall4* (Fig. 1C, D). Meanwhile, THY-1 (CD90), a marker for cell differentiation, dramatically decreased at 7 dpi and remained nearly undetectable in the following reprogramming process (Fig. 1D).

To understand if SMN is functionally correlated with induced cell reprogramming, the exogenous mouse *Smn1* gene was introduced into E13.5 C57BL/6 MEFs along with OSKM factors. In the control group, in which cell reprogramming was induced by only OSKM factors, initial iPSC colonies were not observed until 14 dpi. In contrast, some initial iPSC colonies were observed as early as 7 dpi and compact cell colonies could be found at 14 dpi in the SMN overexpression group (Fig. 2A).

We quantified AP-positive colonies formed in two groups on 28 dpi and found a significant increase in the number of colonies in the SMN overexpression group (Fig. 2B, C). In addition, the expression levels of pluripotent markers, *Nanog* and *Sall4*, were significantly higher in SMN overexpression cells (Fig. 2D).

To further verify whether SMN is required for complete cell reprogramming, we also introduced the construct encoding shRNA for mouse *Smn1* knockdown to MEFs before induction of cell reprogramming with OSKM factors. While the control group, in which MEFs express shRNA targeting luciferase, formed a comparable number of AP colonies to cells introduced with OSKM only, AP-positive colonies were barely found in cells with SMN shRNA (Fig. 2B, C).

Collectively, our findings indicate that upregulation of SMN expression is functionally correlated with cell reprogramming and overexpression of SMN can enhance the cell reprogramming efficiency on the basis of OSKM factors.

hSMN2 partially rescues the loss of mouse SMN1 on pluripotent gene regulation

Patient-specific pluripotent stem cells are considered as a valuable research model for evaluation of therapeutic approaches. Given the essential role of SMN in induced cell reprogramming, it is reasonable to suspect that it would be more difficult to generate SMA patient-derived iPSCs. However, iPSCs have been established from SMA patients, suggesting that a certain amount of SMN2 protein is sufficient to support cell reprogramming in human cells [26].

We attempted to establish iPSCs from an SMA mouse model generated previously [18]. These model mice lack mouse SMN1, but express hSMN2, thereby mimicking human SMA symptoms at different severity levels as the expression levels of hSMN2 may differ from individuals. We collected TTFs from five mice in the same litter for iPSC establishment. Among them, four mice displayed no SMA symptoms and one had a small body size and rotten ears, which are characterized as mild symptoms of the SMA model mouse [18].

We confirmed their genotype with PCR (Fig. 3A). One of the mice with no symptoms was $Smn1^{+/-}$, whereas the rest were $Smn1^{-/-}$. Notably, all model mice expressed *hSMN2* at different levels.

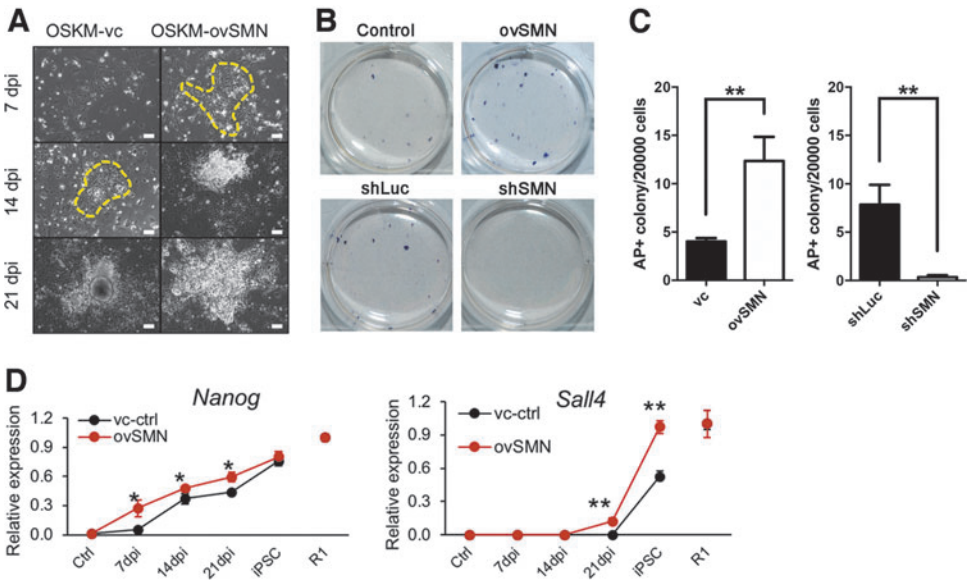

FIG. 2. SMN expression level is positively correlated with cell reprogramming efficiency. **(A)** Images of colonies of cells infected with vector control (OSKM-vc) and the construct encoding SMN (OSKM-ovSMN) at different time points after being infected with constructs encoding OSKM factors. Initial iPSC colonies are indicated with *yellow* dashed lines. Scale bar = 100 μm. **(B)** AP staining for iPSC colonies derived from MEFs infected with control vector (control), the construct encoding SMN (ovSMN), and constructs encoding the shLuc and shSMN group at 28 dpi. ($n = 3$). **(C)** Quantification of AP-positive iPSC colonies in **(B)**. **(D)** mRNA expression levels of *Nanog* and *Sall4* in two groups at different time points after infection ($n = 3$) (Student's *t*-test, $^*P < 0.05$ and $^{**}P < 0.01$). AP, alkaline phosphatase; MEF, mouse embryonic fibroblast; ocSMN, overexpression of SMN; shLuc, luciferase shRNA; shSMN, *Smn1* shRNA.

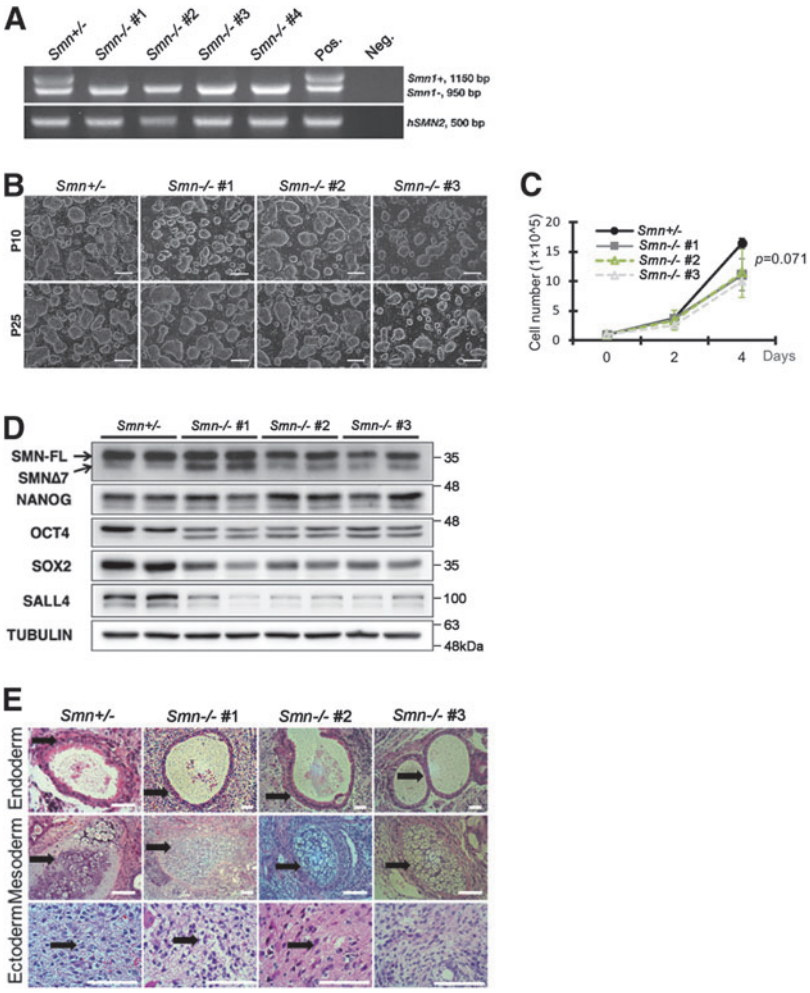

FIG. 3. Characterization of iPSCs derived from *Smn1*$^{-/-}$*/hSMN2* SMA model mice. **(A)** Genotyping results of SMA model mice. Pos. and Neg.: positive and negative controls for PCR analysis, respectively. **(B)** Images of iPSCs derived from *Smn1*$^{+/-}$*/hSMN2* and *Smn1*$^{-/-}$*/hSMN2* mice. No iPSC lines are generated from *Smn1*$^{-/-}$*/hSMN2* No. 4. **(C)** Growth curves of established iPSC lines. **(D)** Western blotting of established iPSC lines for SMN and pluripotent genes. **(E)** H&E-stained sections of teratomas derived from iPSC lines. Tissues of three germ layers are indicated by *arrows*. Scale bar = 50 μm. H&E, hematoxylin and eosin.

OSKM factors were then introduced into these TTFs to induce cell reprogramming. Interestingly, iPSC lines were successfully established from TTFs of four mice without apparent defects, but not from cells of the mouse with mild SMA symptoms, strengthening the notion that SMN is crucial for induced cell reprogramming (Fig. 3B). The colony morphology and cell proliferation were comparable for all four established iPSC lines, and all lines have been cultured for more than 25 passages without apparent morphological changes (Fig. 3B, C).

These findings suggest that the expression of hSMN2 compensates, at least partially, the loss of endogenous SMN1 in iPSCs. Subsequently, we determined the expression levels of SMN and pluripotent genes in these iPSCs with western blotting (Fig. 3D). Notably, mouse SMN1 is only expressed in the *Smn1*$^{+/-}$ iPSCs, while hSMN2 should be expressed in all iPSC lines. The human *SMN2* gene is almost identical to *SMN1*, except that *SMN2* has a single nucleotide difference that results in a truncated unstable protein lacking exon 7 (SMNΔ7) [7].

Therefore, the truncated SMNΔ7 isoform could be an indication for expression of *hSMN2* (Fig. 3D). In these iPSCs, the expression levels of total SMN proteins were generally similar. However, a reduction was seen in the expression levels of SOX2 and SALL4 in three *Smn1*$^{-/-}$ iPSC lines. Moreover, an additional band of OCT4 was displayed by three *Smn1*$^{-/-}$ iPSC lines, suggesting that hSMN2 could not fully restore such defects on splicing of certain transcripts such as *Oct4* in mouse cells.

These again support the notion that the function of SMN is positively correlated with the expression levels of pluripotent genes in iPSCs.

Impeded neuron differentiation in SMA-iPSCs

Given the defects in expression of pluripotent genes, we expected that the differentiation capacity of *Smn1*$^{-/-}$ iPSC lines would be impaired. iPSCs were injected into the hind limb muscles of 6-week-old Nu/Nu mice and teratomas were collected after 3 weeks. Although all three germ layer tissues were found in teratomas derived from *Smn1*$^{+/-}$ and two *Smn1*$^{-/-}$ iPSC lines, one *Smn1*$^{-/-}$ iPSC line (*Smn1*$^{-/-}$ No. 3 iPSCs) failed to differentiate into neuron-like tissues in vivo (Fig. 3E).

We also validated the neuron differentiation capacity of iPSCs by inducing in vitro differentiation. EBs were derived from all four iPSC lines and collected on days 2, 5, 8, and 11 of induction for western blotting. Initially, a higher number of EBs were formed by the heterozygous iPSCs on day 2 (Fig. 4A). However, the morphology of EBs was indistinguishable for all iPSCs from day 5 on.

We analyzed the expression of SMN and genes for neuronal lineage at different points of differentiation. In agreement with previous results, the expression levels of SMN gradually

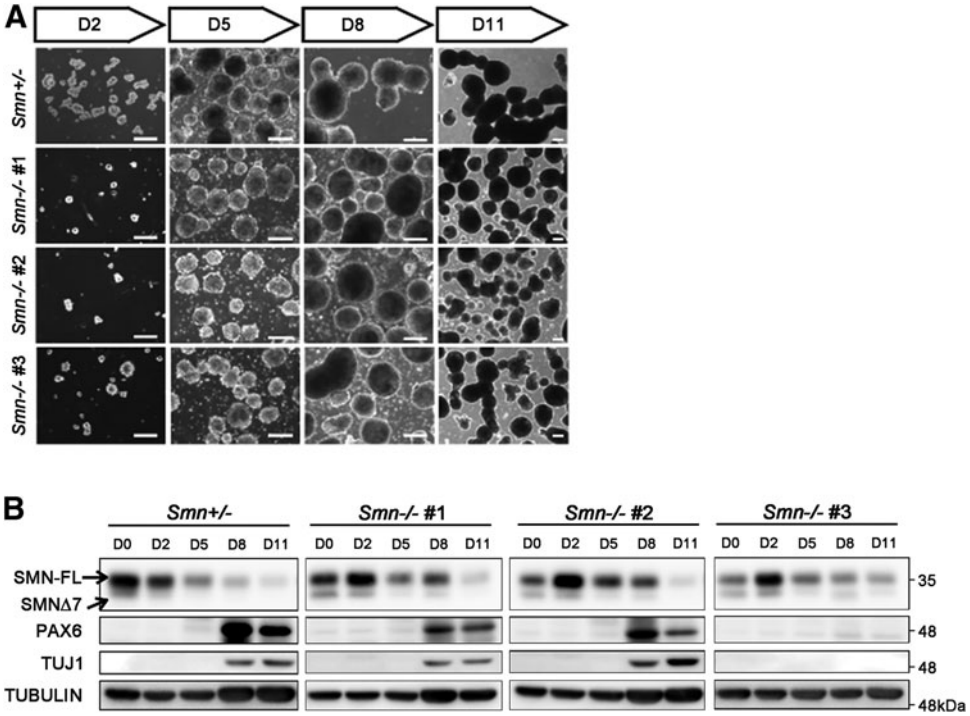

FIG. 4. Loss of mouse SMN in iPSCs may impair neuronal differentiation in vitro. **(A)** Images show the morphology of EBs formed by iPSCs at different time points of differentiation. Scale bar = 200 μm. **(B)** Western blotting of EBs derived from each iPSC line for SMN and the neuronal markers, PAX6 and TUJ1. EBs, embryoid bodies.

decreased throughout differentiation in all iPSC lines, supporting that the expression of SMN positively correlated with pluripotency (Fig. 4B). The expression levels of two neuronal markers, paired box protein (PAX6) and βIII-TUBULIN (TUJ1), were barely detectable before day 8.

In EBs derived from the *Smn1*$^{-/-}$ No. 3 iPSCs, which failed to grow neuron-like tissues in the teratoma, PAX6 and TUJ1 were nearly undetectable throughout the differentiation. These results show consistent defects of *Smn1*$^{-/-}$ No. 3 iPSCs in neuronal lineage differentiation in vivo and in vitro.

Transient overexpression of SMN restores neuronal differentiation capacity of SMA-iPSCs

In the above experiments, we showed that the expression of endogenous SMN would be upregulated along with pluripotent genes during induced cell reprogramming (Fig. 1C, D). Besides, ectopic expression of mouse SMN1 enhanced iPSC derivation efficiency (Fig. 2B, C). We wondered if overexpression of mouse SMN1 could also restore the neuron differentiation capacity of *Smn1*$^{-/-}$ No. 3 iPSCs. We introduced mouse *Smn1*, which is driven by an EF1a promoter, into iPSC lines through lentiviral transduction.

The morphology of iPSC lines overexpressing SMN1 and the control vector are shown in Fig. 5A. Expression levels of pluripotent genes were determined with RT-PCR. In all four iPSC lines, mRNA levels of *Nanog*, *Sall4*, *Rex1*, and *Klf4* were significantly higher in groups overexpressing *Smn1* than that in vector control groups, whereas the levels of *Oct4* and *Sox2* were generally unaffected (Fig. 5B). EB formation was induced in *Smn1*$^{-/-}$ No. 3 iPSC lines, and EBs were collected at different time points for examining neuronal lineage differentiation.

Along with cell differentiation, the levels of SMN gradually reduced in both vector control and *Smn1* overexpression groups (Fig. 5C). Intriguingly, the total SMN levels were not significantly different since day 2, suggesting that the expression of ectopic SMN1 was quickly lost upon cell differentiation.

Despite the loss of SMN1 overexpression, EBs derived from SMN1 overexpression iPSCs started to express the neuronal markers, PAX6 and TUJ1, on day 8, indicating that transient overexpression of SMN1 is sufficient to restore the neuronal differentiation capacity of SMA-iPSCs to a certain extent.

Discussion

Pluripotent stem cells (PSCs), including ESCs and iPSCs, possess great potential in regenerative medicine and are powerful tools for biomedical research [35]. In this study, we show that SMN expression is gradually upregulated during preimplantation mouse embryo development and induced cell reprogramming (Fig. 1). These findings are consistent with our previous works showing that a high amount of SMN is expressed in the inner cell mass of mouse blastocysts and their ESC derivatives [24].

To investigate the functional correlation between SMN and cell reprogramming, we performed gain-of-function and loss-of-function assays in cell reprogramming. While SMN overexpression enhances the reprogramming efficiency under induction with OSKM factors, knockdown of SMN severely impeded iPSC derivation (Fig. 2). These results clearly indicate that the function of SMN is crucial for cell reprogramming.

On the other hand, we attempted to establish iPSC lines from SMA model mice, which resemble symptoms of human SMA patients [17–19]. The human *SMN2* gene is almost identical to *SMN1*, except that *SMN2* has a single nucleotide difference that results in a truncated unstable protein lacking exon 7 (SMNΔ7) [7]. In clinical practice, patients with several copies of SMN2 have a less severe phenotype [36].

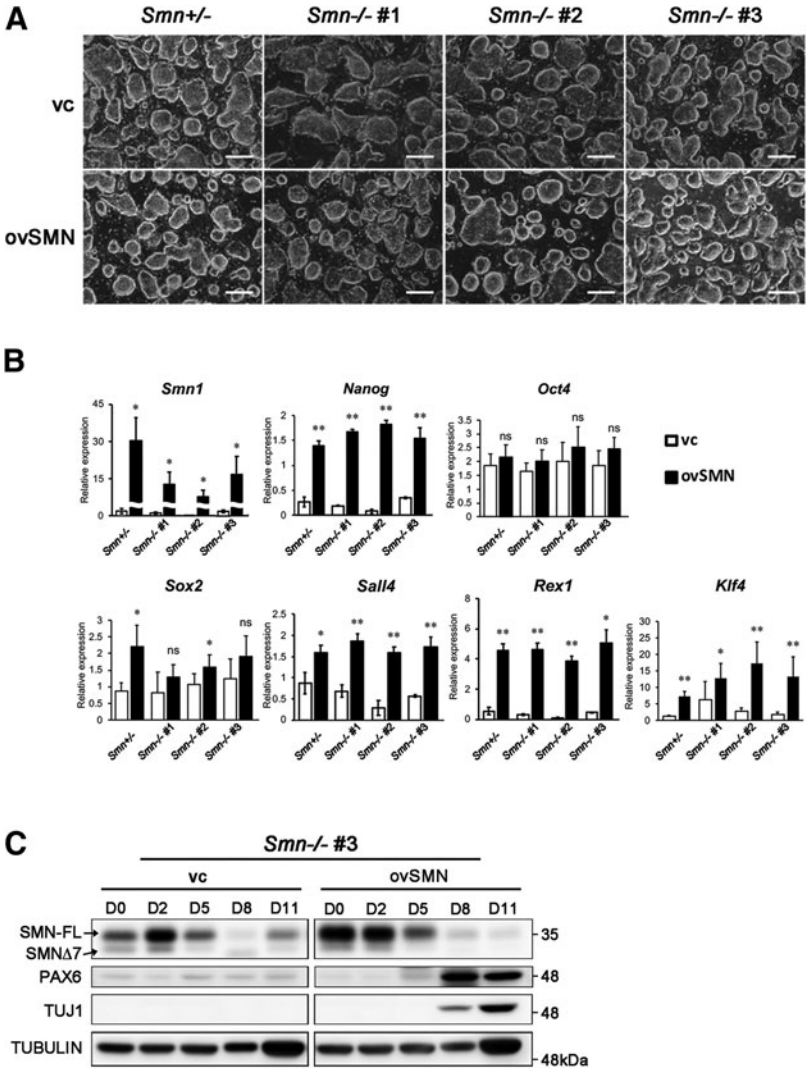

FIG. 5. Overexpression of SMN upregulates expression levels of pluripotent genes in iPSCs and restores the neuronal differentiation capability of SMA-iPSCs. **(A)** Images show the morphology of iPSCs infected with the vc and the ovSMN construct. Scale bar = 200 μm. **(B)** RT-PCR for the expression of *Smn1* and pluripotent genes in vc and ovSMN iPSC lines ($n = 3$). (Student's t-test, $^{*}P < 0.05$ and $^{**}P < 0.01$). **(C)** Western blotting of EBs derived from control and SMN overexpression SMA-iPSCs for SMN and the neuronal markers, PAX6 and TUJ1. ovSMN, overexpression of SMN; vc, control vector.

In all four $Smn^{-/-}$ mice, we successfully derived iPSCs from three mice with no apparent symptoms and failed from the one with mild symptoms, implying that variation in full-length SMN2 levels might affect reprogramming of cells lacking SMN1 (Fig. 3A–D). In addition, the slight differences in levels of SMN proteins may render different neuronal differentiation capacity of iPSCs. Since SMN is a key factor to sustain the development and maturation of motor neurons, and deficiency of SMN leads to degradation and death of neuronal cells, it is not surprising that one of our $Smn1^{-/-}$ iPSC lines ($Smn1^{-/-}$ No. 3 iPSCs) failed to differentiate into neuronal lineage in vitro and in vivo (Figs. 3E and 4B) [36–38].

Such a differentiation defect could be rescued by overexpressing mouse SMN1 in iPSCs (Fig. 5C). The unexpected reduction of exogenous SMN upon cell differentiation shows that a high amount of SMN is not required throughout the differentiation of neuronal cells.

Many factors, such as cell cycle regulators, p53 and p21, or poly (ADP-ribose) polymerase 1 (PARP1) and chromatin regulator DNMTs and Tet1/2, have been shown to affect induced cell reprogramming [39–41]. However, whether RNA splicing regulators are crucial for cell reprogramming remains largely unclear. Recently, changes in alternative splicing were observed during cell reprogramming of B cells and MEFs, implying that splicing factors play pivotal roles in this process [42].

In the current study, we show that SMN may participate in regulation of expression of certain pluripotent genes in iPSCs and possibly also in preimplantation embryos. Our findings suggest additional roles of SMN in embryo development and also propose a potential strategy for enhancing somatic cell reprogramming efficiency with transient overexpression of SMN.

Acknowledgments

The authors would like to thank the Joint Center for Instruments and Researches, College of Bioresources and Agriculture in National Taiwan University, who provided the service for the laser scanning confocal microscopy and RT-PCR machine. The shRNAs were generated and obtained from the National RNAi Core Facility at the Institute of Molecular Biology, Genomic Research Center, Academia Sinica.

Author Disclosure Statement

No competing financial interests exist.

Funding Information

This research was funded by the Ministry of Science and Technology, Taiwan (MOST 106-2313-B-002-039-MY3, MOST 109-2313-B-002-003-MY2 to L.-Y.S., and MOST 110-2811-B-002-624 to W.-F.C.).

References

1. Liu Q and G Dreyfuss. (1996). A novel nuclear structure containing the survival of motor neurons protein. EMBO J 15:3555–3565.
2. Burlet P, C Huber, S Bertrandy, MA Ludosky, I Zwaenepoel, O Clermont, J Roume, AL Delezoide, J Cartaud, A Munnich and S Lefebvre. (1998). The distribution of SMN protein complex in human fetal tissues and its alteration in spinal muscular atrophy. Hum Mol Genet 7: 1927–1933.
3. Renvoise B, K Khoobarry, MC Gendron, C Cibert, L Viollet and S Lefebvre. (2006). Distinct domains of the spinal muscular atrophy protein SMN are required for targeting to Cajal bodies in mammalian cells. J Cell Sci 119: 680–692.
4. Liu JL and JG Gall. (2007). U bodies are cytoplasmic structures that contain uridine-rich small nuclear ribonucleoproteins and associate with P bodies. Proc Natl Acad Sci U S A 104:11655–11659.
5. Matera AG, RM Terns and MP Terns. (2007). Non-coding RNAs: lessons from the small nuclear and small nucleolar RNAs. Nat Rev Mol Cell Biol 8:209–220.
6. Singh RN, MD Howell, EW Ottesen and NN Singh. (2017). Diverse role of survival motor neuron protein. Biochim Biophys Acta Gene Regul Mech 1860:299–315.
7. Lorson CL, E Hahnen, EJ Androphy and B Wirth. (1999). A single nucleotide in the SMN gene regulates splicing and is responsible for spinal muscular atrophy. Proc Natl Acad Sci U S A 96:6307–6311.
8. Lorson CL, H Rindt and M Shababi. (2010). Spinal muscular atrophy: mechanisms and therapeutic strategies. Hum Mol Genet 19:R111–R118.
9. Pearn J. (1978). Incidence, prevalence, and gene frequency studies of chronic childhood spinal muscular atrophy. J Med Genet 15:409–413.
10. Prior TW, PJ Snyder, BD Rink, DK Pearl, RE Pyatt, DC Mihal, T Conlan, B Schmalz, L Montgomery, et al. (2010). Newborn and carrier screening for spinal muscular atrophy. Am J Med Genet A 152A:1608–1616.
11. Sleigh JN, TH Gillingwater and K Talbot. (2011). The contribution of mouse models to understanding the pathogenesis of spinal muscular atrophy. Dis Model Mech 4: 457–467.
12. Briese M, B Esmaeili, S Fraboulet, EC Burt, S Christodoulou, PR Towers, KE Davies and DB Sattelle. (2009). Deletion of smn-1, the *Caenorhabditis elegans* ortholog of the spinal muscular atrophy gene, results in locomotor dysfunction and reduced lifespan. Hum Mol Genet 18:97–104.
13. Chan YB, I Miguel-Aliaga, C Franks, N Thomas, B Trulzsch, DB Sattelle, KE Davies and M van den Heuvel. (2003). Neuromuscular defects in a Drosophila survival motor neuron gene mutant. Hum Mol Genet 12:1367–1376.
14. Chang HC, DN Dimlich, T Yokokura, A Mukherjee, MW Kankel, A Sen, V Sridhar, TA Fulga, AC Hart, D Van Vactor and S Artavanis-Tsakonas. (2008). Modeling spinal muscular atrophy in Drosophila. PLoS One 3:e3209.
15. McWhorter ML, UR Monani, AH Burghes and CE Beattie. (2003). Knockdown of the survival motor neuron (Smn) protein in zebrafish causes defects in motor axon outgrowth and pathfinding. J Cell Biol 162:919–931.
16. Boon KL, S Xiao, ML McWhorter, T Donn, E Wolf-Saxon, MT Bohnsack, CB Moens and CE Beattie. (2009). Zebrafish survival motor neuron mutants exhibit presynaptic neuromuscular junction defects. Hum Mol Genet 18:3615–3625.
17. Frugier T, FD Tiziano, C Cifuentes-Diaz, P Miniou, N Roblot, A Dierich, M Le Meur and J Melki. (2000). Nuclear targeting defect of SMN lacking the C-terminus in a mouse model of spinal muscular atrophy. Hum Mol Genet 9:849–858.
18. Hsieh-Li HM, JG Chang, YJ Jong, MH Wu, NM Wang, CH Tsai and H Li. (2000). A mouse model for spinal muscular atrophy. Nat Genet 24:66–70.
19. Monani UR, M Sendtner, DD Coovert, DW Parsons, C Andreassi, TT Le, S Jablonka, B Schrank, W Rossoll, et al. (2000). The human centromeric survival motor neuron gene (SMN2) rescues embryonic lethality in Smn(-/-) mice and results in a mouse with spinal muscular atrophy. Hum Mol Genet 9:333–339.
20. Ratni H, GM Karp, M Weetall, NA Naryshkin, SV Paushkin, KS Chen, KD McCarthy, H Qi, A Turpoff, et al. (2016). Specific correction of alternative survival motor neuron 2 splicing by small molecules: discovery of a potential novel medicine to treat spinal muscular atrophy. J Med Chem 59:6086–6100.
21. Naryshkin NA, M Weetall, A Dakka, J Narasimhan, X Zhao, Z Feng, KK Ling, GM Karp, H Qi, et al. (2014). Motor neuron disease. SMN2 splicing modifiers improve motor function and longevity in mice with spinal muscular atrophy. Science 345:688–693.
22. Kletzl H, A Marquet, A Gunther, W Tang, J Heuberger, GJ Groeneveld, W Birkhoff, E Mercuri, H Lochmuller, C et al. (2019). The oral splicing modifier RG7800 increases full length survival of motor neuron 2 mRNA and survival of motor neuron protein: results from trials in healthy adults and patients with spinal muscular atrophy. Neuromuscul Disord 29:21–29.
23. Pattali R, Y Mou and XJ Li. (2019). AAV9 Vector: a Novel modality in gene therapy for spinal muscular atrophy. Gene Ther 26:287–295.
24. Chang WF, J Xu, CC Chang, SH Yang, HY Li, HM Hsieh-Li, MH Tsai, SC Wu, WTK Cheng, JL Liu and LY Sung. (2015). SMN is required for the maintenance of embryonic stem cells and neuronal differentiation in mice. Brain Struct Funct 220:1539–1553.
25. Chang WF, J Xu, TY Lin, J Hsu, HM Hsieh-Li, YM Hwu, JL Liu, CH Lu and LY Sung. (2020). Survival motor neuron protein participates in mouse germ cell development and spermatogonium maintenance. Int J Mol Sci 21:794.
26. Ebert AD, J Yu, FF Rose, Jr., VB Mattis, CL Lorson, JA Thomson and CN Svendsen. (2009). Induced pluripotent stem cells from a spinal muscular atrophy patient. Nature 457:277–280.
27. Corti S, M Nizzardo, C Simone, M Falcone, M Nardini, D Ronchi, C Donadoni, S Salani, G Riboldi, et al. (2012). Genetic correction of human induced pluripotent stem cells from patients with spinal muscular atrophy. Sci Transl Med 4:165ra162.
28. Fuller HR, B Mandefro, SL Shirran, AR Gross, AS Kaus, CH Botting, GE Morris and D Sareen. (2015). Spinal

muscular atrophy patient iPSC-derived motor neurons have reduced expression of proteins important in neuronal development. Front Cell Neurosci 9:506.
29. Liu H, J Lu, H Chen, Z Du, XJ Li and SC Zhang. (2015). Spinal muscular atrophy patient-derived motor neurons exhibit hyperexcitability. Sci Rep 5:12189.
30. Nagy A, J Rossant, R Nagy, W Abramow-Newerly and JC Roder. (1993). Derivation of completely cell culture-derived mice from early-passage embryonic stem cells. Proc Natl Acad Sci U S A 90:8424–8428.
31. Morita S, T Kojima and T Kitamura. (2000). Plat-E: an efficient and stable system for transient packaging of retroviruses. Gene Ther 7:1063–1066.
32. Takahashi K and S Yamanaka. (2006). Induction of pluripotent stem cells from mouse embryonic and adult fibroblast cultures by defined factors. Cell 126:663–676.
33. Yamanaka S. (2009). Elite and stochastic models for induced pluripotent stem cell generation. Nature 460:49–52.
34. Wichterle H, I Lieberam, JA Porter and TM Jessell. (2002). Directed differentiation of embryonic stem cells into motor neurons. Cell 110:385–397.
35. Huang CY, CL Liu, CY Ting, YT Chiu, YC Cheng, MW Nicholson and PCH Hsieh. (2019). Human iPSC banking: barriers and opportunities. J Biomed Sci 26:87.
36. Lefebvre S, P Burlet, Q Liu, S Bertrandy, O Clermont, A Munnich, G Dreyfuss and J Melki. (1997). Correlation between severity and SMN protein level in spinal muscular atrophy. Nat Genet 16:265–269.
37. Rossoll W, S Jablonka, C Andreassi, AK Kroning, K Karle, UR Monani and M Sendtner. (2003). Smn, the spinal muscular atrophy-determining gene product, modulates axon growth and localization of beta-actin mRNA in growth cones of motoneurons. J Cell Biol 163:801–812.
38. Fan L and LR Simard. (2002). Survival motor neuron (SMN) protein: role in neurite outgrowth and neuromuscular maturation during neuronal differentiation and development. Hum Mol Genet 11:1605–1614.
39. Piccolo FM, H Bagci, KE Brown, D Landeira, J Soza-Ried, A Feytout, D Mooijman, P Hajkova, HG Leitch, et al. (2013). Different roles for Tet1 and Tet2 proteins in reprogramming-mediated erasure of imprints induced by EGC fusion. Mol Cell 49:1023–1033.
40. Larmonier CB, KW Shehab, D Laubitz, DR Jamwal, FK Ghishan and PR Kiela. (2016). Transcriptional reprogramming and resistance to colonic mucosal injury in poly(ADP-ribose) polymerase 1 (PARP1)-deficient mice. J Biol Chem 291:8918–8930.
41. Secardin L, CEG Limia, A di Stefano, MH Bonamino, J Saliba, K Kataoka, SK Rehen, H Raslova, C Marty, et al. (2020). TET2 haploinsufficiency alters reprogramming into induced pluripotent stem cells. Stem Cell Res 44: 101755.
42. Vivori C, P Papasaikas, R Stadhouders, B Di Stefano, AR Rubio, CB Balaguer, S Generoso, A Mallol, JL Sardina, et al. (2021). Dynamics of alternative splicing during somatic cell reprogramming reveals functions for RNA-binding proteins CPSF3, hnRNP UL1, and TIA1. Genome Biol 22:171.

Address correspondence to:
Li-Ying Sung, PhD
Institute of Biotechnology
National Taiwan University
No. 81, Chang-Xiang Street
Da-an District
Taipei 106
Taiwan

E-mail: liyingsung@ntu.edu.tw

Received for publication April 8, 2022
Accepted after revision July 14, 2022
Prepublished on Liebert Instant Online July 17, 2022